Journal of
Applied
Crystallography

ISSN 0021-8898

Received 15 July 2008
Accepted 24 September 2008

Statistical properties of measured X-ray intensities affected by counting loss

T. Ida

Ceramics Research Laboratory, Nagoya Institute of Technology, Asahigaoka, Tajimi, 507-0071, Japan. Correspondence e-mail: ida.takashi@nitech.ac.jp

The statistical properties of X-ray intensities measured with counting systems have been experimentally investigated. A formula of statistical variance for the intermediately extended dead-time model is proposed and compared with the experimentally evaluated variance obtained from repeated measurements based on Chipman's foil method applied to X-ray detection systems of laboratory and synchrotron powder diffractometers. It has been found that the variance of the observed intensities is smaller than the average of count, as has been suggested by conventional theoretical models for counting loss. It is shown that the statistical errors can be predicted by applying an intermediately extended dead-time model including dead-time τ and degree of extension ρ as fixed parameters.

1. Introduction

The weighted least-squares method is widely applied to analysis of diffraction intensity data. The sum of the squared deviation of each observation from the calculated value can be treated as a maximum-likelihood estimator, where the deviation is weighted by the reciprocal of the known statistical error in the measurement.

It is usually assumed that the statistical error of the X-ray intensity measured by a counting method is identical to the square root of the measured count, which can be justified if the statistical distribution of the counted pulses obeys Poisson statistics. Independently generated signal pulses are certainly expected to obey the Poisson distribution, which predicts that the probability of measuring a number of pulses n during the measurement period T is given by

$$P_{\rm Poisson}(n) = (n!)^{-1}(rT)^n \exp(-rT), \tag{1}$$

where r is the average rate of generated pulses. The mean $\mu_{\rm Poisson}$ and variance $\sigma^2_{\rm Poisson}$ of the Poisson distribution are simply given by $\mu_{\rm Poisson} = \sigma^2_{\rm Poisson} = rT$.

However, it is not expected that the intensities measured with a realistic counting system should strictly obey the Poisson distribution, because they are always affected by counting loss caused by the finite response time of a detector and/or the electronic circuits in the detection system (Omote, 1990).

The mean and variance of the counted pulses based on the non-extended dead-time model with a dead-time τ are approximately given by (Müler, 1974)

$$\mu_{\rm non} = rT/(1 + r\tau), \tag{2}$$

$$\sigma^2_{\rm non} = \mu_{\rm non}/(1 + r\tau)^2, \tag{3}$$

while those predicted by the extended dead-time model are given by

$$\mu_{\rm ext} = rT \exp(-r\tau), \tag{4}$$

$$\sigma^2_{\rm ext} = \mu_{\rm ext}[1 - 2r\tau \exp(-r\tau)]. \tag{5}$$

The validity of the above approximate formulae has recently been confirmed by a systematic investigation based on Monte Carlo simulations (Ida, 2007). This study suggests that the statistical errors of the observed count and the statistical errors to be attached to the corrected intensity data can be evaluated if a detection system is modelled by either the non-extended or the extended dead-time model.

However, no reasonable formulae to predict statistical variance for an intermediately extended dead-time model (Ida & Iwata, 2005) have been reported, despite the fact that it can model experimental behaviours measured with the detailed Chipman (1969) foil method more flexibly than the conventional dead-time models.

In the present study, a hypothetical formula of statistical variance for the intermediately extended dead-time model is proposed and compared with the experimental statistical properties obtained from repeated measurements based on the Chipman foil method applied to X-ray detection systems of laboratory X-ray and synchrotron powder diffractometers.

2. Intermediately extended dead-time model

The intermediately extended dead-time model was originally developed to model the intermediate character of the count-loss behaviour observed for a real X-ray detection system (Ida & Iwata, 2005). The average count $\mu_{\rm int}$ is given by

$$\mu_{\rm int} = f_{\rm ext}\,[f_{\rm non}(r; \tau_1); \tau_2]T, \tag{6}$$

where

$$f_{\rm non}(r;\tau) = r/(1+r\tau) \quad (7)$$

and

$$f_{\rm ext}(r;\tau) = r\exp(-r\tau) \quad (8)$$

are throughput functions for the non-extended and extended dead-time models, respectively.

It is convenient to substitute the total dead-time parameter τ and the degree of extension ρ for the parameters τ_1 and τ_2, *via* the equations

$$\tau \equiv \tau_1 + \tau_2, \quad (9)$$

$$\rho \equiv \tau_2^2/\tau^2, \quad (10)$$

so that the formula exactly gives the non-extended and extended dead-time dependences for $\rho = 0$ and $\rho = 1$, respectively. The throughput function of the model is then expressed by

$$f_{\rm int}(r;\tau,\rho) = f_{\rm ext}\,[f_{\rm non}(r;\tau_1);\tau_2], \quad (11)$$

$$\tau_1 = \tau - \tau_2,$$

$$\tau_2 = \rho^{1/2}\tau.$$

It is also known that the formula given by Ida & Iwata (2005),

$$f_{\rm int'}(r;\tau,\rho) = \begin{cases} t_2^{-1}[\exp(-r_1t_2) - \exp(-2r_1t_2)] & [t_2 \neq 0] \\ r_1 & [t_2 = 0], \end{cases} \quad (12)$$

$$r_1 = r/(1+rt_1),$$

$$t_1 = \tau - 3t_2/2,$$

$$t_2 = (6\rho/13)^{1/2}\tau,$$

is a good approximation for $f_{\rm int}(r;\tau,\rho)$, and an explicit formula for the inverse function of $f_{\rm int'}(r;\tau,\rho)$ is available as

$$f_{\rm int'}^{-1}(m;\tau,\rho) = r_1/(1-r_1t_1), \quad (13)$$

$$r_1 = \begin{cases} -t_2^{-1}\ln\{[1+(1-4mt_2)^{1/2}]/2\} & [t_2 \neq 0] \\ m & [t_2 = 0], \end{cases} \quad (14)$$

where m is the observed count rate.

It should be noted that the formula for $f_{\rm int}(r;\tau,\rho)$ given in equation (11) is not simply the model for a series of two counting devices with non-extended and extended dead-time characters, because the output pulses affected by the non-extended dead-time counting loss cannot be modelled by Poisson statistics, while the formula of equation (8) implicitly assumes the Poisson statistics of the input pulses for the extended dead-time device.

Changing the viewpoint, the formula given by equation (11) would be justified for a hypothetical series of two devices, where the throughput of the first device is given by equation (7) but the output pulses from the first device are still expressed by Poisson statistics, and the second device serially connected to the first device loses counts following the extended dead-time scheme given by equation (8). Then the statistical variance of the intensity measured by the hypothetical series is logically given by

$$\sigma_{\rm int}^2 = r_2T\exp(-r_2\tau_2)\,[1 - 2r_2\tau_2\exp(-r_2\tau_2)], \quad (15)$$

$$r_2 = r/(1+r\tau_1). \quad (16)$$

Even though the above formula of variance for the intermediately extended dead-time model may appear too artificial, it will still be worth trying to compare the values predicted by the model with experimental observations.

3. Experimental

3.1. Laboratory X-ray diffractometer

The counting-loss characteristics of the X-ray detection system of a laboratory powder X-ray diffractometer (Rigaku RAD-2C) were investigated. A Cu $K\alpha$ tube operated at 40 kV and 30 mA was used as the X-ray source. Several aluminium foils were inserted into the beam path to adjust the maximum intensity, which was measured with a scintillation counter. The allowed level of the signal pulses was restricted with a pulse height analyser (PHA) unit to within 26 and 166% relative to the most frequently detected level of pulses.

A home-made mechanism to insert and remove an additional attenuator of nine aluminium foils with 20 µm thickness (180 µm thickness in total) was attached to the diffractometer; this attenuator was remotely operated by the controller for the diffractometer.

A flat single-crystalline plate of α-quartz (001) was placed at the specimen position, and the X-ray intensity was varied in 48 steps by finely scanning the $2\theta/\theta$ axis around the 003 reflection peak located at $2\theta \simeq 26.7°$.

At each intensity step, two sets of measurements of X-ray intensity were obtained, each over a 0.5 s period, repeated 500 times by inserting and 500 times by removing the additional attenuator. This means that the number of unattenuated and attenuated intensity data at each intensity step is $N = 1000$ for each condition. The total measurement time needed to complete the data collection was about 14 h. The time dependence of the measured count observed at a certain intensity data point is shown in Fig. 1.

3.2. Synchrotron powder diffractometer

The counting-loss characteristics of an X-ray detection system of a synchrotron powder diffractometer with multiple detection systems on beamline BL-4B2 at the Photon Factory in Tsukuba (Toraya *et al.*, 1996) were also investigated.

A synchrotron beam monochromated at 0.12 nm with a double Si(111) crystal monochromator and collimated with a cylindrical mirror was used as the X-ray source. Since the electron storage ring was operated in multi-bunch mode during the measurement, the time structure of the synchrotron X-rays is not expected to be significant for the detection system, which has a response time of about 1 µs. The direct beam attenuated with a molybdenum foil with 10 µm thickness was introduced onto a scintillation counter. A mechanism to insert and remove an additional attenuator of 16 Al foils with 12 µm thickness (192 µm thickness in total) was attached on the upstream side on the entrance slit (2.5 mm width, 0.5 mm height) of the diffractometer. The intensity of the X-rays at the detector was varied in 41 steps by rotating stepwise a centre slit of 0.5 mm in height attached to the θ axis. The allowed level of the signal pulses was restricted with a PHA (Rigaku 5320 C1) to within 50 and 150% relative to the most frequently detected level of pulses.

At each intensity step, five sets of measurements of X-ray intensity were obtained, each over a 0.5 s period, repeated 100 times by inserting and 100 times by removing the additional attenuator. The total measurement time needed to complete the data collection was about 12 h. The time dependence of the measured count observed at a certain intensity data point is shown in Fig. 2.

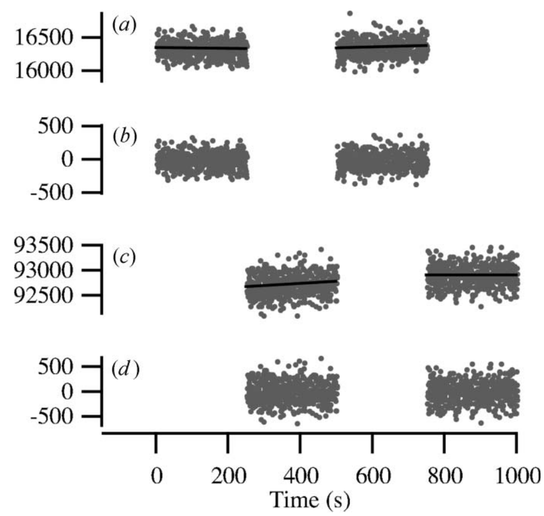

Figure 1
Typical time dependence of intensities measured by the repeated Chipman method for the laboratory powder X-ray diffractometer. (*a*) Attenuated intensities (grey dots) and fitted segmented linear dependence (solid lines), (*b*) residuals of the fit shown in (*a*), (*c*) unattenuated intensities (grey dots) and fitted segmented linear dependence (solid lines), and (*d*) residuals of the fit shown in (*c*).

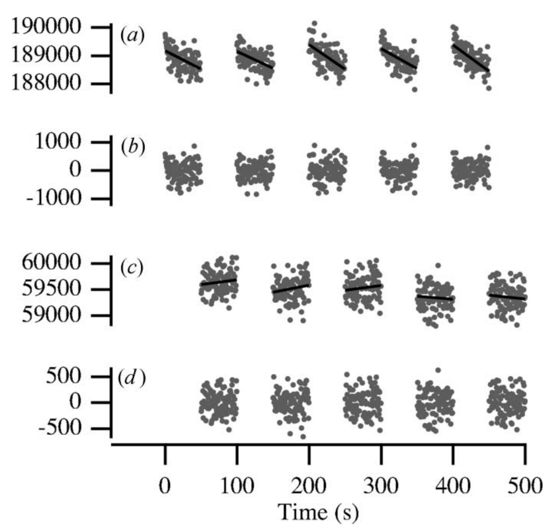

Figure 2
Typical time dependence of intensities measured by Chipman measurements for the synchrotron powder diffractometer. See Fig. 1 for definitions.

4. Results and discussions

4.1. Analysis of data collected with laboratory diffractometer

Since the number of counts observed for the laboratory diffractometer has shown slight time dependence, as can be seen in Fig. 1, a segmented linear dependence has been fitted to the observed intensities, and the variance of residuals is treated as the modified statistical variance of the measured intensity. No significant time dependence has been observed in the values of residuals.

The mean, variance of raw data and variance of residuals for the intensities measured on removal of the additional attenuator (unattenuated intensities) are plotted *versus* the average count measured on insertion of the additional attenuator (attenuated intensities) in Fig. 3.

The values of mean m, variance of raw data v and variance of residuals s for the intensity data sets $\{y_i\}$ $(i = 1, \ldots, N)$ are, respectively, calculated as

$$m = N^{-1} \sum_{i=1}^{N} y_i, \tag{17}$$

$$v = \sum_{i=1}^{N} (y_i - m)^2/(N-1), \tag{18}$$

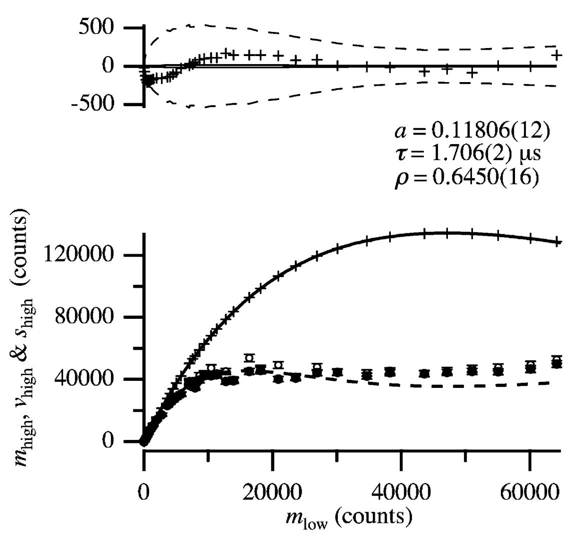

Figure 3
Results of repeated Chipman measurements for the laboratory powder X-ray diffractometer. Lower panel: average unattenuated intensities $m_{\rm high}$ (crosses), variance of raw data $v_{\rm high}$ (open circles), variance of residuals $s_{\rm high}$ (solid circles), fitting curve for $m_{\rm high}$ based on an intermediately extended dead-time model (solid line), and variance calculated with the optimized parameters (broken line) plotted *versus* average attenuated intensities $m_{\rm low}$. Upper panel: residuals of fitting (crosses) and statistical errors about the average (solid lines, see text), and the errors estimated for a single Chipman measurement (broken lines).

$$s = \sum_{i=1}^{N} [y_i - g(t_i; a_1, \ldots, a_P)]^2/(N-P), \tag{19}$$

where $g(t; a_1, \ldots, a_P)$ is a function with P parameters to optimize the segmented linear dependence on the time t.

The errors for the above expectation values are, respectively, estimated by

$$\Delta m = \left[\sum_{i=1}^{N} \frac{(y_i - m)^2}{N(N-1)}\right]^{1/2}, \tag{20}$$

$$\Delta v = \left[\sum_{i=1}^{N} \frac{(y_i - m)^4}{N^2} - \frac{N-3}{N(N-1)} v^2\right]^{1/2}, \tag{21}$$

$$\Delta s = \left\{\sum_{i=1}^{N} \frac{\left[y_i - g(t_i; a_1, \ldots a_P)\right]^4}{N^2} - \frac{s^2}{N}\right\}^{1/2}. \tag{22}$$

The dependence of the mean unattenuated intensities $m_{\rm high}$ upon the attenuated intensities $m_{\rm low}$ is fitted by using an approximate formula for the intermediately extended dead-time model (Ida & Iwata, 2005), given by

$$m_{\rm high} = f_{\rm int'}[f_{\rm int'}^{-1}(m_{\rm low}/T; \tau, \rho)/a; \tau, \rho]T, \tag{23}$$

where a is the transmittance of the additional attenuator.

The observed dependence of $m_{\rm high}$ *versus* $m_{\rm low}$ is fairly well reproduced by the model with the optimized values of transmittance $a = 0.11806\,(12)$, dead-time $\tau = 1.706\,(2)\,\mu$s and degree of extension $\rho = 0.6450\,(16)$.

It is also concluded that the dependence is not completely modelled by equation (23), as the residuals plotted as crosses in the upper panel of Fig. 3 show a systematic deviation larger than the estimated statistical errors of the average count, drawn as solid lines (which are almost coincident with the zero line owing to their small values). The errors of intensities estimated for a single Chipman measurement, simply calculated by multiplication of the errors for the average by $(N-1)^{1/2} = 999^{1/2}$, are shown as broken lines in the upper panel of Fig. 3. The figure demonstrates that the incompleteness of the model would not appear significant if data collected by a single Chipman measurement were used to evaluate the parameters a, τ and ρ in equation (23).

The plot of the observed variance, $v_{\rm high}$ and $s_{\rm high}$, in Fig. 3 clearly indicates that the variance evaluated by the repeated measurements is systematically smaller than the average $m_{\rm high}$, as has been predicted by the conventional theoretical models for counting loss of detection systems (Müler, 1974).

The curve calculated by equation (15) with the values of a, τ and ρ optimized to fit the mean values is drawn as a broken line in Fig. 3. The observed values of variance are slightly larger than the values calculated by the intermediately extended dead-time model, which appears more significant in the higher count rate regions. The slight difference still seems reasonable, because the model does not include any other origins than the segmented linear time dependence for the variation of the source X-ray intensities.

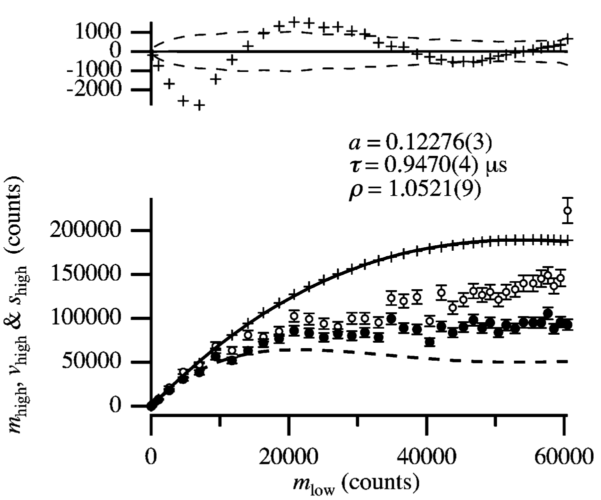

Figure 4
Results of repeated Chipman measurements for the synchrotron powder diffractometer. See Fig. 3 for definitions.

4.2. Analysis of data collected with synchrotron diffractometer

The number of counts observed for the synchrotron diffractometer has shown a more significant time dependence than that for the laboratory diffractometer, as can be seen in Fig. 2. The data shown in Fig. 2 were measured at the highest intensity point in the series of measurements, and the amplitude of the periodic time dependence was about 0.05% relative to the average value. The gradual decrease in intensity may be attributed to the decay of the synchrotron beam supplied from the storage ring, while the origin of the periodic behaviour is not clear. A segmented linear dependence has been fitted to the observed intensities, and the variance of residuals is treated as the modified statistical variance of measured intensity, similarly to the analysis of the data collected with the laboratory diffractometer. No significant time dependence could be found in the values of residuals.

The mean $m_{\rm high}$, variance of raw data $v_{\rm high}$ and variance of residuals $s_{\rm high}$ of the intensities measured on removal of the additional attenuator (unattenuated intensities) are plotted *versus* the average count $m_{\rm low}$ measured on insertion of the additional attenuator (attenuated intensities) in Fig. 4.

The dependence of the mean unattenuated intensities $m_{\rm high}$ on the attenuated intensities $m_{\rm low}$ is well fitted by equation (23), with the optimized parameters of transmittance $a = 0.12276\,(3)$, dead-time $\tau = 0.9470\,(4)\,\mu$s and degree of extension $\rho = 1.0521\,(9)$. The observed dependence is not completely modelled by equation (23), as the residuals plotted in the upper panel of Fig. 4 show systematic deviation larger than the statistical errors, similarly to the results for the laboratory diffractometer.

The dependence of raw variance $v_{\rm high}$ on $m_{\rm low}$ shows a large dispersion, as can be seen at the highest intensity point in Fig. 4, while the dependence of $s_{\rm high}$ is found to be almost smooth within the estimated errors $\Delta s_{\rm high}$. This figure suggests that most of the periodic time dependence shown in Fig. 2 has been removed by subtracting the segmented linear dependence.

Table 1
True count rate r, observed count rate r_{obs} (both in counts per second), variance of observed count $(\Delta r_{obs}T)^2$ and variance of corrected count $(\Delta r_c T)^2$, predicted for the laboratory diffractometer with a dead-time $\tau = 1.706$ µs and degree of extension $\rho = 0.6450$.

r	r_{obs}	$(\Delta r_{obs}T)^2$	$(\Delta r_c T)^2$
300	300	300	300
1000	998	996	1002
3000	2985	2960	3022
1×10^4	0.983×10^4	0.957×10^4	1.024×10^4
3×10^4	2.852×10^4	2.629×10^4	3.226×10^4
1×10^5	0.847×10^4	0.651×10^5	1.286×10^5
3×10^5	1.876×10^5	0.912×10^5	7.194×10^5

Table 2
Count rate (counts per second) and variance predicted for the synchrotron diffractometer with a dead-time $\tau = 0.947$ µs and degree of extension $\rho = 1.052$.

r	r_{obs}	$(\Delta r_{obs}T)^2$	$(\Delta r_c T)^2$
300	300	300	300
1000	999	997	1001
3000	2991	2974	3008
1×10^4	0.991×10^4	0.972×10^4	1.009×10^4
3×10^4	2.916×10^4	2.751×10^4	3.085×10^4
1×10^5	0.909×10^4	0.749×10^5	1.106×10^5
3×10^5	2.253×10^5	1.267×10^5	4.434×10^5

The curve calculated by equation (15) with the values of a, τ and ρ optimized to fit the mean values is drawn as a broken line in Fig. 4. Even though the experimental variances have been estimated at larger values than the calculated curve, the variance of residuals s_{high} approaches closer to the calculated curve than the raw variance v_{high}. Since the time-dependent variation of the source X-ray intensities is not likely to be fully modelled by the segmented linear dependence, it is suggested that the statistical variance calculated by equation (15) still gives an appropriate description of the statistical variance of the measured count.

4.3. Correction of counting loss

When the dead-time τ and the degree of extension ρ are known, the corrected count rate r_c can be calculated from the observed count rate $r_{obs} = m/T$ by applying the following equation:

$$r_c = f_{int'}^{-1}(r_{obs}; \tau, \rho). \qquad (24)$$

Statistical errors for the corrected count rate, Δr_c, can be calculated by

$$\Delta r_c = \Delta r_{obs}(dr_c/dr_{obs}) = \Delta r_{obs}(dr_{obs}/dr_c)^{-1}, \qquad (25)$$

where

$$(\Delta r_{obs})^2 = r_2 T^{-1} \exp(-r_2\tau_2)\,[1 - 2r_2\tau_2 \exp(-r_2\tau_2)], \qquad (26)$$

$$r_2 = r_c/(1 + r_c\tau_1), \qquad (27)$$

$$dr_{obs}/dr_c = (dr_2/dr_c)\,(1 - r_2\tau_2)\exp(-r_2\tau_2), \qquad (28)$$

$$dr_2/dr_c = 1/(1 + r_c\tau_1)^2. \qquad (29)$$

It should be noted that the error Δr_c for the corrected count rate r_c diverges to infinity when the count rate approaches the inverse of the dead time τ^{-1}.

Tables 1 and 2 list the expected observed count rate, r_{obs}, and the variances of the observed and corrected intensities, $(\Delta r_{obs}T)^2$ and $(\Delta r_c T)^2$, for several values of true count rate r, calculated using the parameters estimated in §§4.1 and 4.2 for the laboratory and synchrotron diffractometers.

The statistical variance of the corrected intensity $(\Delta r_c T)^2$ is close to the average count in the low count rate region, whereas it shows a rapid increase when the true count rate r approaches the reciprocal of the dead-time τ of the detection system. This result indicates that the correction for statistical errors is necessary on application of the weighted least-squares method as a maximum-likelihood estimation, especially in the high count rate region.

5. Conclusion

The statistical properties of X-ray intensities measured with laboratory and synchrotron powder diffractometers have been experimentally investigated. Repeated application of Chipman's method has revealed that the statistical variance of the observed intensity, affected by counting loss of the detection system, is lower than the average, as has been suggested by conventional theoretical models for counting loss.

The statistical errors can be evaluated for any observed intensity by applying the intermediately extended dead-time model including dead-time τ and degree of extension ρ as fixed parameters.

Part of this work has been performed under the approval of the Photon Factory Program Advisory Committee (proposal No. 2007 G093).

References

Chipman, D. R. (1969). *Acta Cryst.* A**25**, 209–214.
Ida, T. (2007). *J. Appl. Cryst.* **40**, 964–965.
Ida, T. & Iwata, Y. (2005). *J. Appl. Cryst.* **38**, 426–432.
Müler, J. W. (1974). *Nucl. Instrum. Methods*, **117** 401–404.
Omote, K. (1990). *Nucl. Instrum. Methods Phys. Res. Sect. A*, **293**, 582–588.
Toraya, H., Hibino, H. & Ohsumi, K. (1996). *J. Synchrotron Rad.* **3**, 75–83.